Disrupting Inflammation-Associated CXCL8-CXCR1 Signaling Inhibits Tumorigenicity Initiated by Sporadic- and Colitis-Colon Cancer Stem Cells[1]

Robert C. Fisher[*], Kishan Bellamkonda[*], L. Alex Molina[*], Shao Xiang[*], David Liska[*,†], Samaneh K. Sarvestani[*], Susmita Chakrabarti[‡], Annamarie Berg[*], Marda L. Jorgensen[§], Denise Hatala[¶], Sugong Chen[#], Alexandra Aiello[**], Henry D. Appelman[††], Edward W. Scott[‡‡] and Emina H. Huang[*,†]

[*]Department of Stem Cell Biology and Regenerative Medicine, Lerner Research Institute, Cleveland Clinic, Cleveland, OH, USA; [†]Department of Colorectal Surgery, Cleveland Clinic, Cleveland, OH, USA; [‡]Department of Molecular Cardiology, Cleveland Clinic, Cleveland, OH, USA; [§]Department of Pediatrics, University of Florida, Gainesville, Florida, USA; [¶]Immunochemistry Core, Lerner Research Institute, Cleveland Clinic, Cleveland, OH, USA; [#]Department of Surgery, Duke University Medical Center, Durham, North Carolina, USA; [**]Quantitative Health Sciences, Cleveland Clinic, Cleveland, OH, USA; [††]Department of Pathology, University of Michigan, Ann Arbor, MI, USA; [‡‡]Department of Molecular Genetics and Microbiology, University of Florida, Gainesville, Florida, USA

Abstract

Dysfunctional inflammatory pathways are associated with an increased risk of cancer, including colorectal cancer. We have previously identified and enriched for a self-renewing, colon cancer stem cell (CCSC) subpopulation in primary sporadic colorectal cancers (CRC) and a related subpopulation in ulcerative colitis (UC) patients defined by the stem cell marker, aldehyde dehydrogenase (ALDH). Subsequent work demonstrated that CCSC-initiated tumors are dependent on the inflammatory chemokine, CXCL8, a known inducer of tumor proliferation, angiogenesis and invasion. Here, we use RNA interference to target CXCL8 and its receptor, CXCR1, to establish the existence of a functional signaling pathway promoting tumor growth initiated by sporadic and colitis CCSCs. Knocking down either CXCL8 or CXCR1 had a dramatic effect on inhibiting both *in vitro* proliferation and angiogenesis. Likewise, tumorigenicity was significantly inhibited due to reduced levels of proliferation and angiogenesis. Decreased expression of cycle cell regulators cyclins D1 and B1 along with increased p21 levels suggested that the reduction in tumor growth is due to dysregulation of cell cycle progression. Therapeutically targeting the CXCL8-CXCR1 signaling pathway has the potential to block sustained tumorigenesis by inhibiting both CCSC- and pCCSC-induced proliferation and angiogenesis.

Introduction

Growing evidence suggests that cancer is an inflammatory disease with sporadic colorectal cancer and the evolution from chronic colitis to colitis-associated cancer as vivid examples [1]. The exact mechanisms of how inflammation potentiates colon cancer initiation and progression remain unclear. However, exposure of normal colonic epithelium to chronic inflammation in the form of soluble mediators secreted by immune cells and stromal fibroblasts is thought to play an essential early role in both CRC and CAC progression

models [2,3]. Additional events for both colon cancer progression models include epigenetic and genetic alterations of intrinsic drivers of tumorigenesis including oncogenic and gain-of-function mutations that are required for colon cancer progression [4,5].

CRCs contain a minor subpopulation of cancer stem cells (colon cancer stem cells; CCSCs) that resemble normal colonic stem cells based on their ability to self-renew and display multipotency upon differentiation [6–8]. However, in contrast to normal colonic stem cells, CCSCs possess enhanced survival and the unique ability to initiate the formation of tumors. We have isolated highly enriched CCSC sphere isolates from sporadic CRC patients using ALDH enzymatic activity [9] and related sphere isolates from UC patients [10]. The stem cell-associated properties are maintained during *in vitro* propagation of the primary sphere isolates. This feature highlights their value for mechanistic- and discovery-based studies examining CCSC-mediated tumor initiation and progression along with elucidating the pathogenesis of CAC [11,12].

Initial *in vivo* characterization of a model CCSC sphere isolate demonstrated that tumor growth was dependent on the inflammatory chemokine, CXCL8 [10]. CXCL8 is a member of the CXC chemokine family and expressed primarily by inflammation-associated immune cells and a select subset of cancer cells [13]. Besides mediating inflammatory responses, CXCL8 is important for promoting tumorigenesis-associated proliferation, angiogenesis and invasion. CXCL8 binds to two highly related receptors, CXCR1 and CXCR2. CXCR1 binds ligands including CXCL6 and CXCL8, while the more promiscuous CXCR2 binds CXCL1, CXCL2, CXCL3, CXCL5, CXCL6, CXCL7 and CXCL8. Both receptors have been proposed to stimulate unique signals following CXCL8 binding, which may be due to key binding site amino acid residues differing between CXCR1 and CXCR2 [14,15]. Notably, CXCL8 lacks a murine orthologue, which further highlights the functional importance of our CCSC models in defining the role of CXCL8-CXCR1 signaling in tumorigenesis [16].

In this study, we hypothesize that autocrine CXCL8-CXCR1 signaling plays an essential role in controlling the capacity of long-term CCSCs to sustain tumorigenesis. Using RNA interference and a combination of *in vitro* and *in vivo* functional assays, we confirmed that disrupting the CXCL8-CXCR1 signaling pathway utilized by long-term CCSCs resulted in reduced tumor growth due to inhibition of cell cycle progression and tumor angiogenesis. Overexpression of CXCL8 and CXCR1 in CRC and UC patient tissues validated the significance of our functional studies. Collectively, these findings merit the further development of therapeutics targeting the CXC8-CXCR1 pathway as a strategy to inhibit the capacity of long-term CCSCs to promote tumorigenesis.

Material and Methods

Human Specimens and CCSC Primary Sphere Isolates

Tissues from UC patients and sporadic CRC patients were retrieved under pathologic supervision with Institutional Review Board approvals at the University of Michigan, University of Florida and the Cleveland Clinic (Supplementary Table 1). ALDEFLUOR-High primary sphere isolates were derived from UC and CRC colonic tissue and cultured in serum-free defined medium (DM) [10]. The CRC sphere isolate used in this study, CA2, functionally represents a sporadic CCSC, while the UC sphere isolates, CT1, functionally represents a colitis CCSC [11]. These isolates were selected based on their ability to be propagated both *in vitro* and *in vivo*. Short tandem

repeat analysis (Duke University DNA Analysis Facility, Durham, North Carolina; DDC Medical, Fairfield, Ohio) was performed using genomic DNA isolated from sphere isolates (DNeasy Tissue Kit; Qiagen; 69,506) and corresponding primary tissue (Wax Free DNA Extraction Kit; TrimGen Genetic Technology; WF-100) to establish the genetic identity.

Animals and Tumor Xenografts

Non-obese diabetic mice, severe combined immunodeficiency, IL2γ receptor null male and female mice (NSG mice, Jackson Laboratory, Bar Harbor, Maine; 005557) maintained under pathogen-free conditions were used. Experiments were approved by the Institutional Animal Care Committee at the University of Florida and the Cleveland Clinic Lerner Research Institute. *In vivo* limiting dilution assays [9] were used to confirm the long-term, self-renewing potential of ALDEFLUOR-enriched CA2 CCSC [17] and the CT1 CCSC (Supplementary Table 4). Primary and secondary (2°) tumor xenografts were generated as previously described [11]. Briefly, cancer stem cell suspension cultures, either control or KD, were enriched for 10% highest level of expression of TurboGFP (FACS Aria, Becton-Dickinson), indicating inclusion of the construct, then inoculated subcutaneously into the flanks of NSG mice (100 cells in 100 µl Matrigel). Once these tumors grew to a minimum of 5 mm in any single dimension, they were harvested, dissociated, and again the 10% highest level of expression of TurboGFP was selected for inoculation (100 cells in 100 µl Matrigel). Tumors were then measured bi-weekly with calipers. Volumes were calculated using the formula $length^2 \times width$, in which length was the greatest dimension. Tumors were harvested when no greater than 100 mm^3 to prevent central necrosis, which would impair detection of BrdU incorporation.

Generation of Stable shRNA-expressing CCSC and pCCSC Primary Sphere Isolates

SMARTvector 2.0 lentiviral shRNA particles targeting CXCL8 (shCXCL8–2, SH-004756-02-10, TCCGTAATTCAACACAGCA and shCXCL8–3, SH-004756-03-10, TATGCACTGACATC-TAAGT), CXCR1/IL8RA (shCXCR1–1, SH-005646-01, TGGCGATGATCACAACAT and shCXCR1–3, SH-005646-03, TGTACGCAGGGTGAATCCA) and a non-targeting control (shNT; S01–005000-01) were purchased from Dharmacon, Horizon Discovery. CA2 CCSC and CT1 pCCSC sphere isolates were transduced in the presence of 6 µg/ml hexadimethrine bromide (Millipore Sigma; 107689) for 12 hours. Cells underwent puromycin selection (1.0–2.5 µg/mL; Sigma-Aldrich; P9620) for at least 7 days.

Generation of Conditioned Media (CM) from Sphere Isolates and Primary Tissues

CM was prepared from trypsinized shNT, shIL8/CXCL8 and shCXCR1 transduced cells cultured in low attachment tissue culture plates (Corning; 3471) [10]. CM was prepared from primary colonic tissues (8–25 mg range) incubated for 12 hours. CXCL8 levels in CM samples were quantified using a RayBio Human IL-8 ELISA Kit (ELH-IL8) following the manufacturer's instructions.

CXCR1 Flow Cytometry

shNT, shCXCL8 and shCXCR1 shRNA expressing CA2 CCSC and pCCSC cells were dissociated for 20 minutes using accutase (Millipore; SCR005), washed 2× in 1× D-PBS and incubated with Human TruStain FcX (BioLegend; 422302; 10 µL/5 × 10^5 cells) for 15 minutes at 25 °C. Samples (1–2 × 10^5 cells) were incubated with

anti-human CXCR1-PE murine mAb (R&D Systems; FAB33OP) or mouse IgG2a-PE control mAb (Abcam; ab91363) for 30 minutes at 4 °C. Samples were washed 2× with 1× D-PBS containing 1% BSA (Roche; 03 116 956 001). DAPI was added and CXCR1$^+$/DAPI$^-$ were detected using an LSRFortessa Cell Analyzer (BD Biosciences; San Jose, CA; BD FACSDiva software, version 8.0) and acquired data was analyzed by FlowJo (version 9.9.6). Gating was performed on unstained cells to exclude cell debris and aggregates. DAPI$^-$ cells were gated to select for viable cells.

CXCR1 Immunoblotting

Transduced shNT, and shCXCR1 CCSCs and pCCSCs were harvested, washed three times with 1× D-PBS, resuspended in 100 µL 20 mM HEPES (pH 7.4), 2 mM $MgCl_2$, 1 mM EDTA (pH 7.4) containing protease inhibitors (Roche Diagnostics; 0589791001), and sheared 15 times through a 26-gauge needle. The cell lysates were centrifuged at 3,000 rpm (4 °C) for 5 minutes. The supernatants were saved and analyzed by immunoblotting [17]. CXCR1 was detected using an anti-human CXCR1 antibody (Abcam; ab139955; 1:1000). CXCR1 protein levels were normalized to GAPDH [17].

BrdU Proliferation Assay

Cell proliferation assays were performed on trypsinized shNT, shCXCL8 and shCXCR1 transduced CCSCs or pCCSCs [17] and measured using a BrdU ELISA (Roche Diagnostics; 11 669 915001) according to manufacturer's instructions.

Methylcellulose Colony Formation Assay

Colony formation assays were performed on trypsinized shNT, shCXCL8 and shCXCR1 transduced CCSCs or pCCSCs [17]. Five random brightfield images were documented per assay plate using a Leica DM1600 microscope at 5× magnification or an EVOS XL Core Cell Imaging System (Electron Microscopy Sciences; Hatfield, PA) at 4× magnification. The resulting images were quantified for colonies >50 µm using Image J software.

HUVEC Tube Formation Assay

Human umbilical vein endothelial cells (HUVEC; Invitrogen; C-003-5C) were maintained *in vitro* using Vasculife VEGF Complete Medium (LifeLine Cell Technology; LS-0002). HUVECs were trypsinized and resuspended in shRNA NT or shRNA CXCL8 CM samples. Resuspended cells were plated (10,000 cells/50 µL) in an ibidi Angiogenesis u-Slide (*ibid* GmbH; 81506) containing 10 µL/well of Matrigel (BS Biosciences; 354234) and incubated at 37 °C/5% CO_2. Five random images were documented at 6 hours by bright field microscopy using a Leica DM1600 or DM3000 microscopes at 5× magnification. Tube length was quantified using ImageJ software.

Immunochemistry

Immunochemical analyses of tumor xenograft sections were performed [18] using a Ventana Discovery ULTRA automated stainer (Ventana Medical Systems Inc.; Tucson AZ) for the following primary antibodies: CXCR1, CXCL8, Cyclin D1, Cyclin B1 and p21. Detection of BrdU incorporation and tumor vessel density were performed manually [18]. See Supplementary Table 4 for additional details. CXCR1 immunoreactivity analysis of CRC, UC, and normal human primary colonic tissues was performed using an anti-human CXCR1 antibody as described in Supplementary Table 4. The slides were evaluated by an expert pathologic reviewer (HDA) blinded to the clinicopathologic details. A combined "immunoreactivity score" was calculated based on the percentage of CXCR1 positive epithelia (none = 0; < 10% = 1; 10–50% = 2; 51–80% = 3; > 80% = 4) and the intensity of the staining (none = 0; weak = 1; moderate = 2; strong = 3) [19]. Slides with a DAB readout were scanned using a Leica SCN400F slide scanner (20× magnification) and representative images were documented using a Leica DM4000B microscope (40× magnification; Leica 7000 T camera; Leica LAS X software). Depending on the size of the tumor section, 250-to-2000 nuclei-positive colonic epithelia cells were quantified using ImageJ software. MECA-32 stained tumor sections were documented and quantified [18].

Statistics

Student's *t* test was used for comparisons using Graphpad Prism 7. For tumorigenicity studies, all analyses were performed using SAS (version 9.4, The SAS Institute, Gary, NC). Oncomine© (Compendia Bioscience, Ann Arbor, MI) data sets were displayed as Kaplan–Meier survival curves and compared by log-rank test using Graphpad Prism 7. For all analyses, $P < .05$ was considered statistically significant.

Results

### CXCR1 and CXCL8 Expression is Elevated in Colitis and Colon Cancer Compared to Normal Colon

We first compared the expression of CXCL8 and CXCR1 in primary normal and diseased tissues from patients with CRC and UC. The immunochemistry panels in Figure 1A demonstrate higher expression of CXCR1 in the epithelia for both CRC (CA24) and UC (CT6) compared to normal colonic epithelium. Consistent with the clinical observation that UC is an inflammatory condition, we observed a significantly higher CXCR1 immunoreactivity score for colitic epithelium compared to normal colon and sporadic CRC epithelia (Figure 1B and Supplementary Table 1; [19]). Compared to normal colon, sporadic CRC epithelium also exhibited a significantly higher CXCR1 immunoreactivity score (Figure 1B and Supplementary Table 1). We next measured the secreted levels of CXCL8, in conditioned media (CM) generated from primary normal, CRC and UC colonic tissues [10]. The CXCL8 concentrations for cancer and colitis tissues were elevated compared to normal colon tissues (Figure 1C and Supplementary Table 2). To further clarify the clinical significance of elevated CXCR1 and CXCL8 levels in sporadic CRC patients, Kaplan–Meier survival analysis was undertaken by comparing median survival time for patients based on the cancer stem cell marker, ALDH1 (Figure 1D, Oncomine© [20], Reid data set) as well as for CXCL8 (Figure 1E, Oncomine© [20], Kurashina data set). For both CXCR1 and CXCL8 there was a difference in survival for ALDH1^{High} patients stratified for CXCR1 or CXCL8 expression. For CXCL8, the survival was significant with $P < .04$, while for CXCR1, $P = .12$, indicative of trend in increased survival for this subset of patients. Thus, CXCR1 and CXCL8 are elevated in both CRC and UC patients and correlate with cancer survival.

CCSCs Demonstrated a Dose-Dependent Proliferative Response to CXCL8 In Vitro

To confirm that sporadic CCSC and colitis CCSC sphere isolates represent a suitable experimental model for studying CXCL8 signaling, we examined the ability of the sphere isolates to proliferate in response to increasing concentrations of exogenous CXCL8 using an *in vitro*, serum-free, colony formation assay (CFA). As shown in Figure 2, A and B, the CRC CCSC primary sphere isolate, CA2,
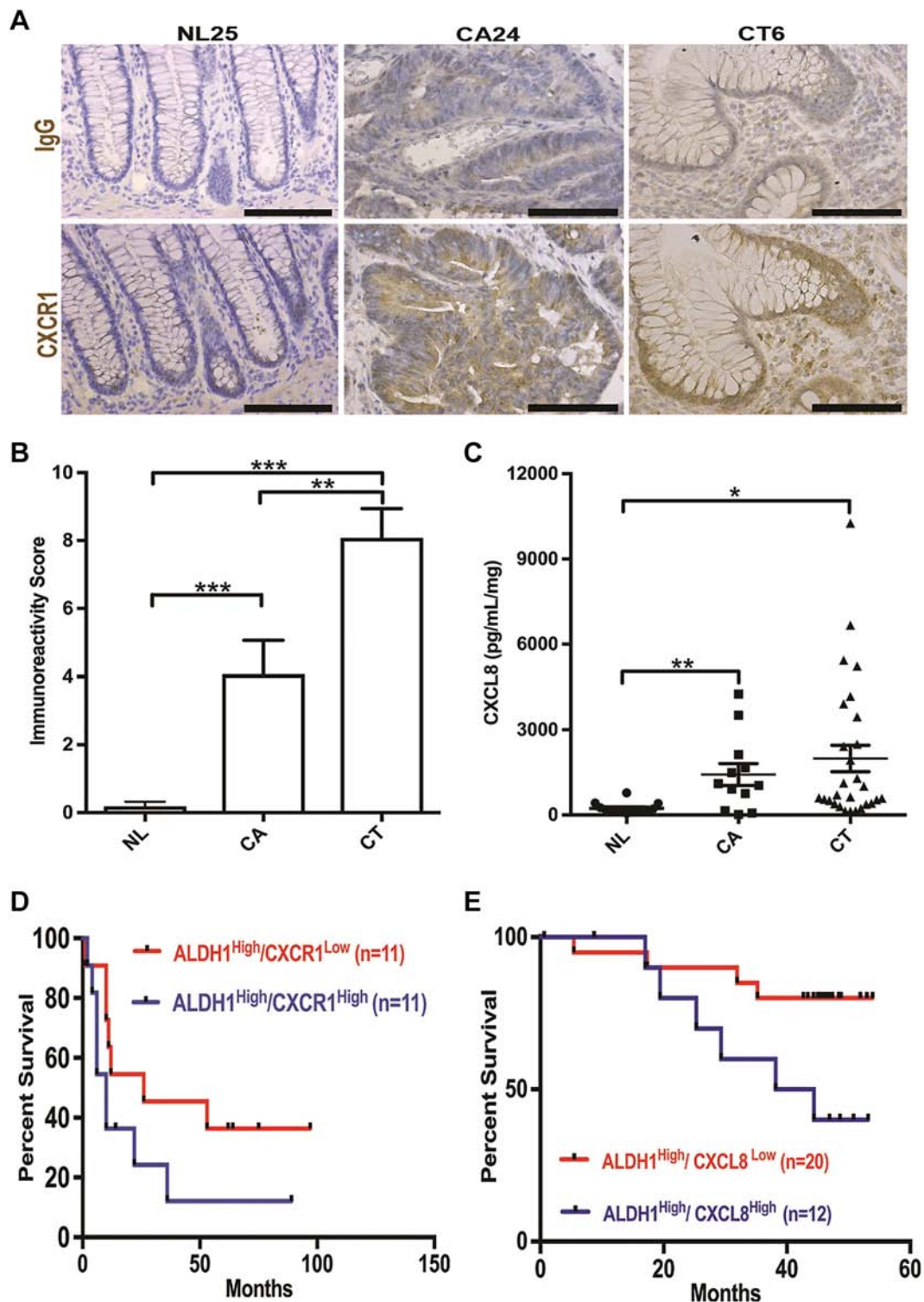
Figure 1. Overexpression of CXCR1 and CXCL8 in CRC and UC patients. Reduced survival for colorectal cancer patients expressing the cancer stem cell marker aldehyde dehydrogenase and high levels of either CXCR1 or CXCL8. **A.** Representative CXCR1 IHC images (bottom panels) for normal colon (NL25), CRC (CA24) and UC (CT6) tissues. Corresponding IgG IHC control images are shown in top panels. CXCR1 and IgG, brown (DAB). **B.** Immunoreactivity score indicating CXCR1 expression levels for normal colonic tissue (NL, $n = 14$) versus CRC (CA, $n = 12$) and UC (CT, $n = 10$). See Supplementary Table 1 for patient characteristics and immunoreactivity index values. **C.** Secretion of CXCL8 (pg/mL/mg; in conditioned media, CM) comparing CRC (CA, $n = 13$), UC (CT, $n = 28$) tissues versus normal colonic tissues (NL, n = 13). See Supplementary Table 2 for patient characteristics and CXCL8 secretion values. **D.** Kaplan–Meier survival curve analysis comparing ALDH1[High] tumors stratified as CXCR1[High] and CXCR1[Low] in CRC patients (Reid data set, Oncomine©; $P = .12$, log-rank test; [20]. **E.** Kaplan–Meier survival curve analysis comparing ALDH1[High] tumors stratified as CXCL8[High] and CXCL8[Low] in CRC patients (Kurashina data set, Oncomine© [20], $P = .0382$, log-rank test). Mean $+/-$ SEM; $*P < .05$, $**P < .01$, $***P < .001$. Scale bars, 100 μm.
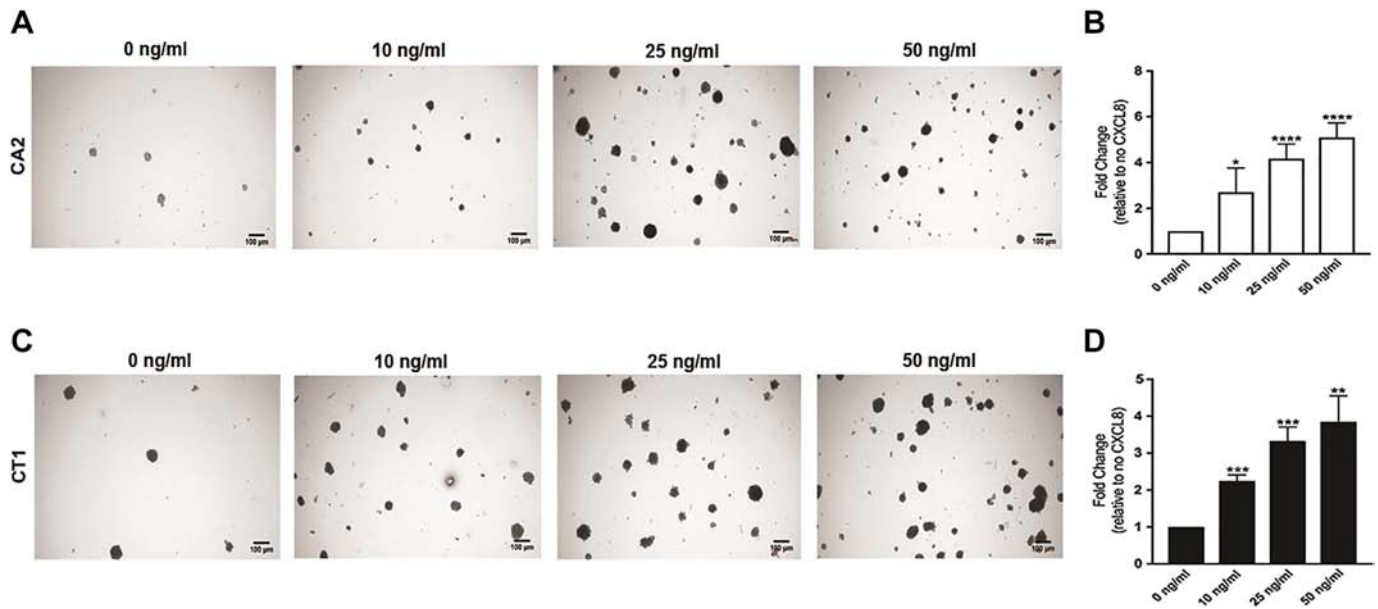
Figure 2. CA2 CCSCs and CT1 CCSCs demonstrate a dose-dependent proliferative response to CXCL8 *in vitro*. Day 14 Colony formation assays were performed with growth factor-starved CA2 CCSCs and CT1 CCSCs with addition of increasing amounts of exogenous CXCL8 (0 ng/mL, 10 ng/mL, 25 ng/mL and 50 ng/mL; $n = 3$). Day 14 representative images are displayed for CA2 CCSCs (**A**) and CT1 CCSCs (**C**). **B and D**. Results are presented as fold-change in total number of colonies relative to absence of exogenous CXCL8 for CA2 CCSCs (**B**) and CT1 pCCSCs (**D**). Open bars: CA2 CCSCs, Filled bars: CT1 CCSCs; Mean $+/-$ SD; $**P < .01$, $***P < .001$, $****P < .0001$. Scale bars, 100 μm.
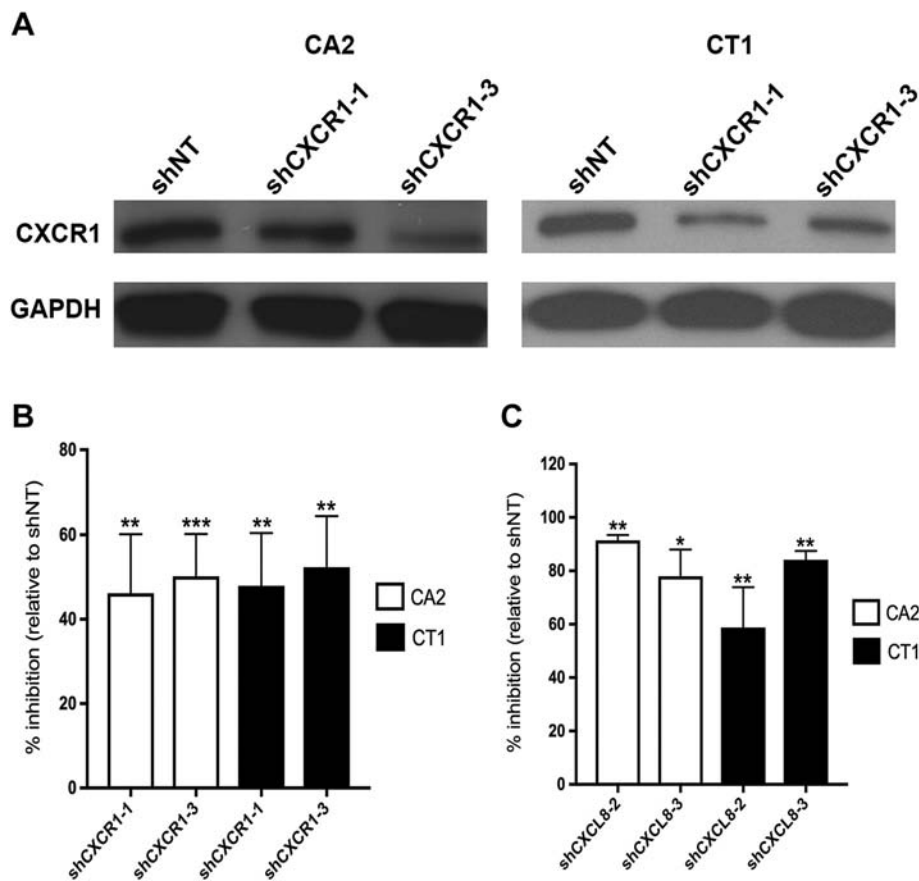

Figure 3. CXCL8 and CXCR1 shRNA expressing CCSCs (CA2) and pCCSCs (CT1) exhibit reduced levels of CXCL8 and CXCR1. **A.** Immunoblotting analysis of CXCR1 and GAPHD expression levels in CA2 CCSC and CT1 CCSC expressing control shRNA (shNT) and shRNAs targeting CXCR1 (shCXCR1–1 and shCXCR1–3). Representative images, $n = 3$. **B.** % inhibition of CXCR1 shRNAs on CXCR1 expression in CA2 CCSC and CT1 CCSCs. Mean $+/-$ SD, $n = 3$; $*P < .05$, $** P < .01$. **C.** CXCL8 ELISA analysis of 24 hours CM samples prepared from control (shNT, $n = 3$) and CXCL8 (shCXCL8–2 and shCXCL8–3, $n = 3$) shRNA expressing CA2 CCSCs and CT1 CCSCs. Results are displayed as % inhibition in secreted CXCL8 levels relative to shNT for CA2 CCSCs and CT1 CCSCs. Open bars: CA2 CCSCs, Filled bars: CT1 pCCSCs; Mean $+/-$ SD; $*P < .05$, $**P < .01$.

proliferated to increasing concentrations of CXCL8 in a dose-dependent manner. A similar dose-dependent response was shown in Figure 2, *C* and *D* by the UC pCCSC primary isolate, CT1. These results demonstrate that both the CA2 CCSCs and CT1 CCSCs proliferate in response to CXCL8.

In Vitro shRNA-Mediated RNA Interference Decreased Expression of CXCL8 and CXCR1 in both Sporadic CCSC and Colitis CCSC Sphere Isolates

Having shown that both CXCL8 and CXCR1 are over expressed in CRC and UC patients, and that primary patient sphere isolates
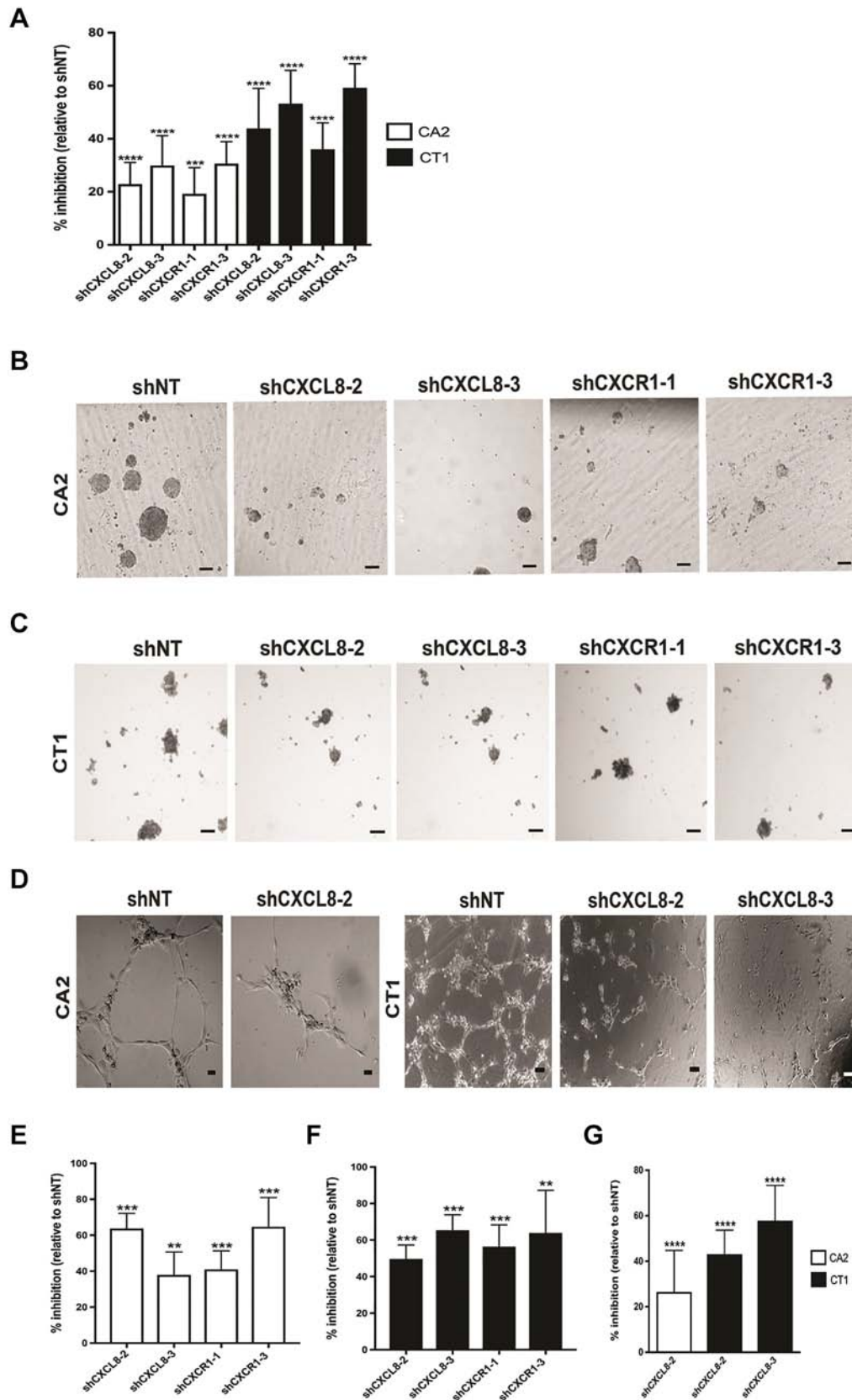
responded to CXCL8 *in vitro* (Figures 1 and 2), we proceeded to functionally test our hypothesis by using RNA interference to knockdown CXCL8 and CXCR1 levels in the CA2 CCSC- and CT1 CCSC- sphere isolates. Lentiviral expression vectors expressing two different shRNAs targeting either CXCL8 (shCXCL8–2, shCXCL8–3), CXCR1 (shCXCR1–1, shCXCR1–3) or a non-targeting control (shNT) were used to stably transduce CA2 CCSCs and CT1 CCSCs.

To validate the knockdown of CXCR1, immunoblotting was used (Figure 3; Supplementary Figure 1). There was a significant decrease in CXCR1 protein expression for the CA2 CCSC (Figure 3*A*, left panels, and B) and the CT1 CCSC (Figure 3*A*, right panels, and B) transductants. To confirm the knockdown of CXCR1, flow cytometry was used (Supplementary Figure 3) [21]. Both of the shRNAs significantly reduced surface expression of CXCR1 by the CA2 CCSC (Supplementary Figure 3, *A* and *C*) and CT1 CCSC (Supplementary Figure 3, *B* and *D*) stable transductants.

Knockdown of CXCL8 was validated by measuring CXCL8 concentrations in 24-hour CM for the CA2 CCSC and CT1 CCSC stable shCXCL8 transductants. The results for the two different CXCL8 shRNAs (shCXCL8–2 and shCXCL8–3) are shown in Figure 3, *C*. For both the CA2 CCSC and CT1 CCSC transductants, there was a significant decrease in CXCL8 levels. Collectively, these results demonstrated that two different shRNAs targeting CXCL8 and CXCR1 can significantly decrease CXCL8 and CXCR1 expression levels, respectively.

Knockdown of CXCL8 or CXCR1 Inhibited in Vitro Proliferation and Angiogenesis

Having established that CXCL8 and CXCR1 are significantly knocked down in both our CRC CCSCs and UC CCSCs, we next proceeded to determine the effect on known *in vitro* functions of CXCL8, which include stimulating proliferation and angiogenesis. First, we examined the effect on proliferation using a serum-free, bulk culture, 96-well plate growth assay. After 5 days, the number of cycling cells in S phase responding to endogenous levels of CXCL8 was measured by the incorporation of BrdU. As demonstrated in Figure 4, *A*, two different shRNAs targeting CXCL8 (CXCL8–2 and CXCL8–3) and CXCR1 (CXCR1–1 and CXCR1–3) were able to significantly inhibit incorporation of BrdU in both the CA2 CCSCs and CT1 CCSCs. We next asked whether decreasing the level of endogenous CXCL8 or its receptor, CXCR1, would reduce *in vitro* proliferation using a serum-free CFA. As shown in Figure 4, *B* and *E*, targeting either CXCL8 or CXCR1 significantly reduced the number of CA2 CCSC colonies for the CXCL8 and CXCR1 knockdowns. Similar results were obtained for CT1 CCSCs for the CXCL8 and CXCR1 knockdowns (Figure 4, *C* and *F*).

Angiogenesis is a known function stimulated by CXCL8 [22,23]. To examine the effect of reduced levels of secreted CXCL8 on

inducing angiogenesis, CM samples from CA2 CCSC and CT1 CCSC transductants were analyzed for angiogenic potential using a human umbilical vein endothelial cells (HUVEC) *in vitro* tube formation assay [24]. As shown in Figure 4, *D* and *G*, shCXCL8–2 had the effect of decreasing the level of CXCL8-induced angiogenesis by CA2 CCSC and CT1 CCSC CM samples. A second shRNA (shCXCL8–3) inhibited the angiogenic potential of the CT1 CCSCs. Taken together, these *in vitro* results support our hypothesis that a CXCL8-CXCR1 autocrine circuit plays a functionally important role for CA2 sporadic CCSC and CT1 colitic CCSC primary sphere isolates by regulating cell proliferation and angiogenesis.

Knockdown of CXCL8 or CXCR1 Expression Inhibits Tumor Growth and Angiogenesis In Vivo

To validate the significance of our *in vitro* results establishing that CXCL8 and CXCR1 contribute to the proliferation of long-term-sporadic CCSCs and –colitic CCSCs, and their respective angiogenic-inducing potential, 100 cells of control (shNT) and CXCL8 and CXCR1 knockdown CT1 CCSCs and CA2 CCSCs were injected into NSG mice to generate secondary (2°) tumor xenografts. The use of 2° tumors significantly decreases the contribution of the short-term, progenitor-like colon cancer initiator cells to tumorigenesis [11,24]. We initiated our *in vivo* tumorigenesis assays with our best-characterized sphere isolate, CA2 [10,18]. The CA2 CCSC tumor growth plots comparing the shNT control tumors *versus* the CXCL8- and CXCR1-knockdown tumors are shown in Figure 5*A*. Comparative statistical analysis for each CA2 CCSC knockdown tumor is denoted in Figure 5*B*. Expression of either shCXCL8–2 or shCXCR1–3 RNA resulted in a trend towards reduced growth (Figure 5, *A* and *B*; left panels). With these results, we extended our *in vivo* study by focusing on the CT1 CCSC sphere isolate by testing additional shCXCL8- and shCXCR1-knockdown CCSCs. For both the CT1 CXCL8- and CXCR1–3-knockdown CCSCs, the decrease in tumorigenicity was significant or approached significance (Figure 5, *A* and *B*, middle and right panels). The expression of CXCL8 in CA2 CCSC- and CT1 CCSC- CXCL8 knockdown tumors and CXCR1 in the CA2 CCSC- and CT1 CCSC-CXCR1 knockdown tumors were analyzed by immunochemistry and shown to be significantly decreased or approached significance (Supplementary Figure 3, *A–C*).

To evaluate whether the decrement in tumorigenicity was due to an effect on proliferation, the levels of BrdU incorporation were determined. For both the CA2 CCSC- and CT1 CCSC- knockdown tumors, shRNAs targeting either CXCL8 or CXCR1 resulted in significantly less BrdU incorporation compared to the shNT control (Figure 5, *C* and *E*). To determine the contribution of the CXCL8-CXCR1 autocrine circuit to tumor angiogenesis, expression of the murine panendothelial marker, MECA-32, was used to quantify blood vessel density (Figure 5D). In parallel with the decrease in

Figure 4. Knockdown of CXCL8 and CXCR1 expression in CA2 CCSCs and CT1 CCSCs decreases *in vitro* proliferation and angiogenesis. **A**. Day 5 BrdU proliferation assay comparing control (shNT, n = 3) *versus* CXCL8 (shCXCL8–2 and shCXCL8, n = 3) and CXCR1 (shCXCR1–1 and shCXCR1–3, n = 3) shRNA-expressing CA2 CCSCs and CT1 CCSCs. Results are presented as % inhibition relative to shNT. **B** and **C**. Representative images of Day 14 colony formation assays comparing control (shNT, n = 3) *versus* CXCL8 (shCXCL8–2 and shCXCL8–3, n = 3) and CXCR1 (shCXCR1–1 and shCXCR1–3, n = 3) shRNA-expressing CA2 CCSCs (**B**) and CT1 (**C**) CCSCs. **E** and **F**. Results are summarized as % inhibition relative to shRNA for CA2 CCSCs (**E**) and CT1 CCSCs (**F**). **D**. HUVEC tube formation assay comparing angiogenic activity in CM prepared from control (shNT) *versus* CXCL8 shRNA-expressing CA2 CCSCs (shCXCL8–2) and CT1 CCSCs (shCXCL8–2 and shCXCL8–3) cells. Representative images are displayed for CA2 (shNT and shCXCL8–2) and CT1 (shNT, shCXCL8–2 and shCXCL8–3). **G**. Results are presented as % inhibition of tube length relative to shNT for CA2 CCSCs and CT1 CCSCs CM samples (n = 3). Open bars: CA2 CCSCs, Filled bars: CT1 pCCSCs: Mean +/− SD; ***P < .001. Scale bars, 100 μm.
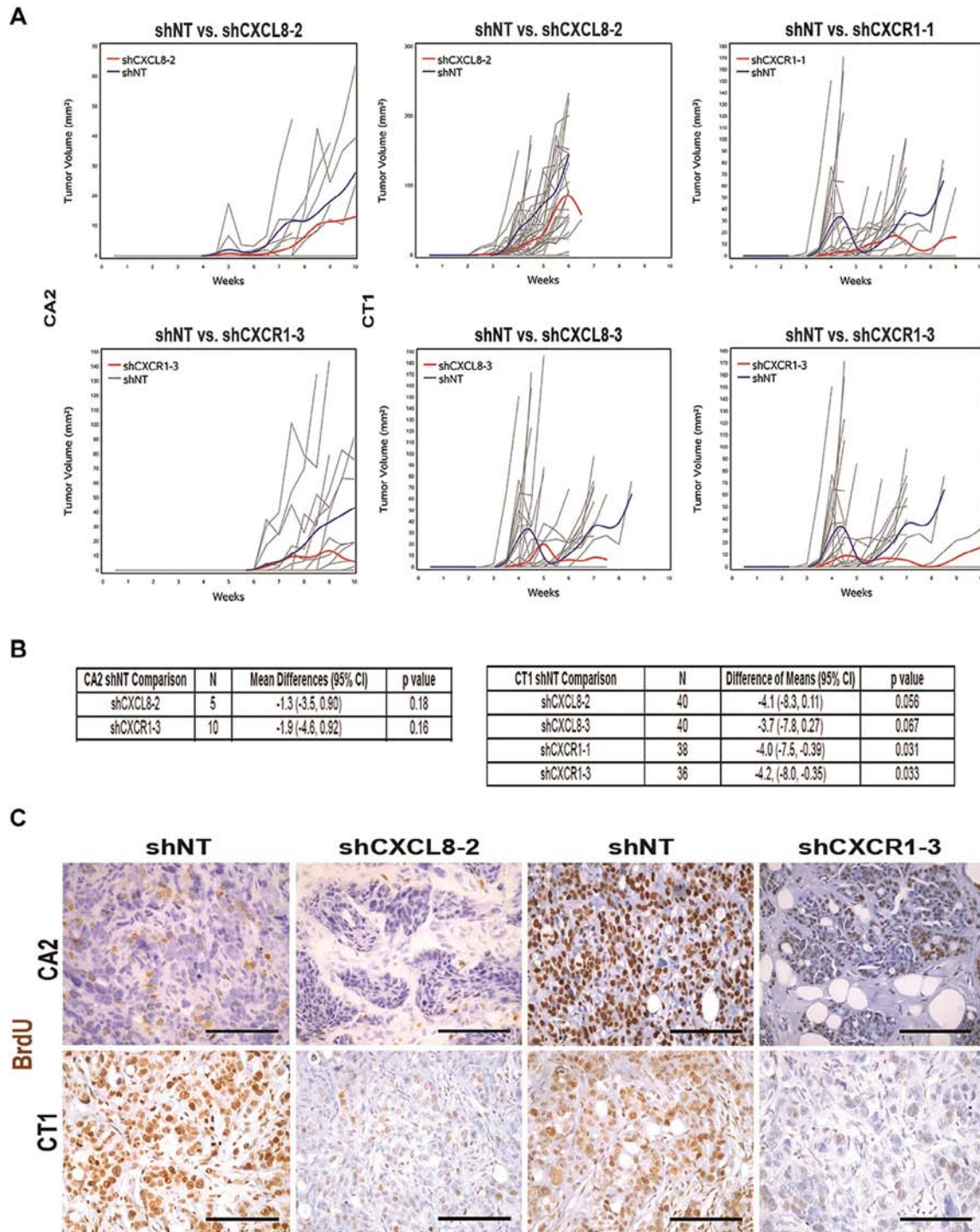
Figure 5. Knockdown of CXCL8 or CXCR1 expression in CA2 CCSCs and CT1 CCSCs inhibits tumorigenesis. **A**. 2° tumor xenograft growth curves comparing shNT *versus* knockdown (CA2 CCSCs); shNT *versus* knockdowns (CT1 CCSCs). Tumors are measured biweekly (mm^3) and represented as a distinct growth curve. Trend lines for the shNT control tumors (mean, blue) *versus* knockdown tumors (red). **B**. Average change in tumor volume between measurements. Paired *t* test compare mean growth changes for CA2 samples (left table; shCXCL8–2, shCXCR1–3, n ≥ 10). Unpaired *t* test results compare mean growth changes for CT1 samples (right table; shCXCL8–2, shCXCL8–3, shCXCR1–1, shCXCR1–3; *n* ≥ 38). **C**. Detection of BrdU incorporation (IHC) as a measure of *in vivo* proliferation to compare CA2 CCSCs and CT1 CCSCs control *versus* knockdown 2° tumor xenografts. Representative shNT, shCXCL8–2 and shCXCR1–3 tumor sections are displayed for CA2 CCSCs (upper panels) and CT1 CCSCs (lower panels). BrdU incorporation, brown. **D.** Meca-32 IHC of murine endothelium to compare the level of tumor angiogenesis in CA2 CCSCs and CT1 pCCSCs knockdown 2° tumor xenografts. Representative shNT and knockdown tumor sections are displayed for CA2 CCSCs (upper) and CT1 CCSCs (lower). MECA-32, red; DAPI, blue **E**. BrdU incorporation levels were quantified and expressed as % inhibition relative to shNT. **F**. Meca-32 expression was quantified and expressed as % inhibition of vessel density relative to shNT. Open bars: CA2 CCSCs, Filled bars: CT1 CCSCs; Mean +/− SD, *n* = 3; *P < .05, **P < .01, ***P < .001, ****P < .0001. Scale bars, 100 μm.
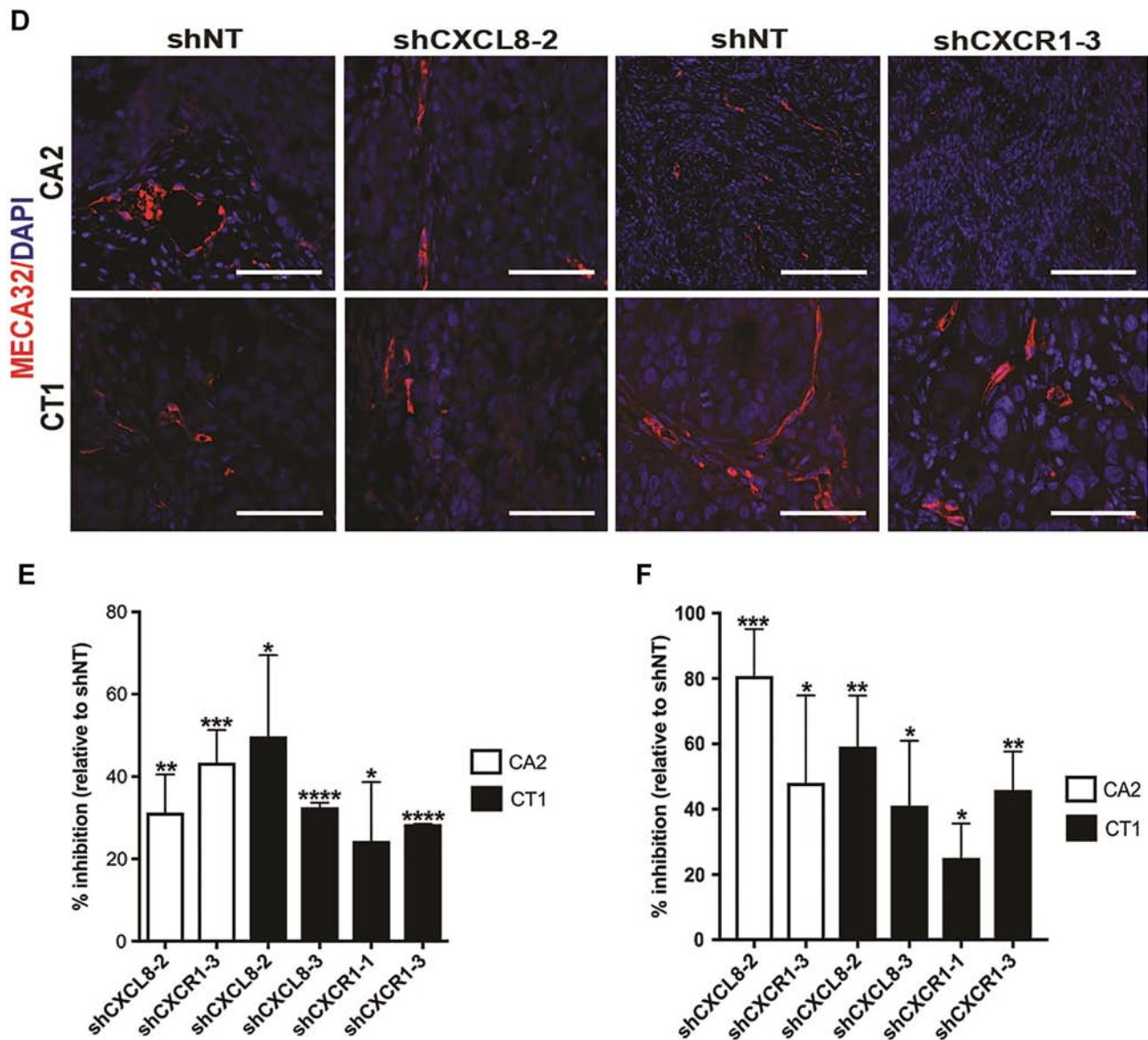
Figure 5. (*continued.*)

tumorigenic responses, the density of MECA-32$^+$ expression was significantly reduced in corresponding to decreased levels of CXCL8 or CXCR1 (Figure 5F). To summarize, when either CXCL8 or CXCR1 levels in the sporadic CCSC or colitic CCSCs are reduced, the decrease in both BrdU incorporation and blood vessel density is consistent with a diminished tumorigenicity, and validated an *in vivo* role for autocrine CXCL8-CXCR1 signaling in regulating tumor proliferation and angiogenesis.

Knockdown of CXCL8 and CXCR1 Dysregulated Expression of Cyclins D1 and B1, and CDK Inhibitor Protein, P21

Transition through the cell cycle is highly regulated and mediated by the levels of cyclin-dependent kinase (CDK)-cyclin complexes [26]. RNA interference-based targeting of CXCL8 and CXCR1 in prostate cancer model cell lines had demonstrated a decrease in the expression of cell cycle regulatory proteins, cyclins D1 and B1 [27,28]. To determine if expression of cyclins D1 and B1 is reduced in the CXCL8- and CXCR1- knockdown tumors, immunochemical analysis was performed. As shown in Figure 6, *A* and *B*, cyclin D1 expression is reduced to varying levels for the CA2 CCSC knockdown

tumors and significantly reduced for the majority of the CT1 CCSC knockdown tumors (Figure 6, *A* and *D*). Figure 6, *C* and *D* display variable levels of reduction of cyclin B1 for both CA2 CCSC knockdown tumors and significant reduction of cyclin B1 for the CT1 CCSC knockdown tumors.

Dysregulation of CDK inhibitory proteins, including p21, can alter the levels of CDK-cyclin complexes [29]. P21 levels have been reported to be increased in response to RNA interference-mediated knockdown of CXCR1 in a prostate cancer cell line model [27]. Based on the findings of this study, immunochemical analysis was performed to determine the expression of p21 in the CXCL8 and CXCR1 knockdown tumors. As shown in Figure 6, *E* and *F*, there is a variable increase in p21 for both the CA2 CCSC, shCXCL8–2- and shCXCR1–3- knockdown tumors. For CT1 CCSCs, p21 is significantly increased in both the shCXCL8–2 and shCXCR1–3 knockdown tumors. In conclusion, a reduction in autocrine CXCL8-CXCR1 signaling decreased the expression of cyclins D1 and B1 and increased the level of p21, and suggest that cell cycle progression is disrupted in the CCSC-initiated knockdown tumors.

Discussion

For sporadic colon cancer, we have reported the use of the ALDEFLUOR assay for the isolation and continued propagation of colon cancer stem cells [9]. Furthermore, in CAC, for which the pathogenesis of tumorigenicity is unclear, we have previously reported the existence of colitis-associated cancer stem cells [10,11] best approached using the ALDEFLUOR assay. Tumor initiation, spawned or perpetuated by cancer stem cells, remain key events in the pathogenesis of CAC; since this progression has an extended prodrome, new targets which may mitigate the progression must be identified.
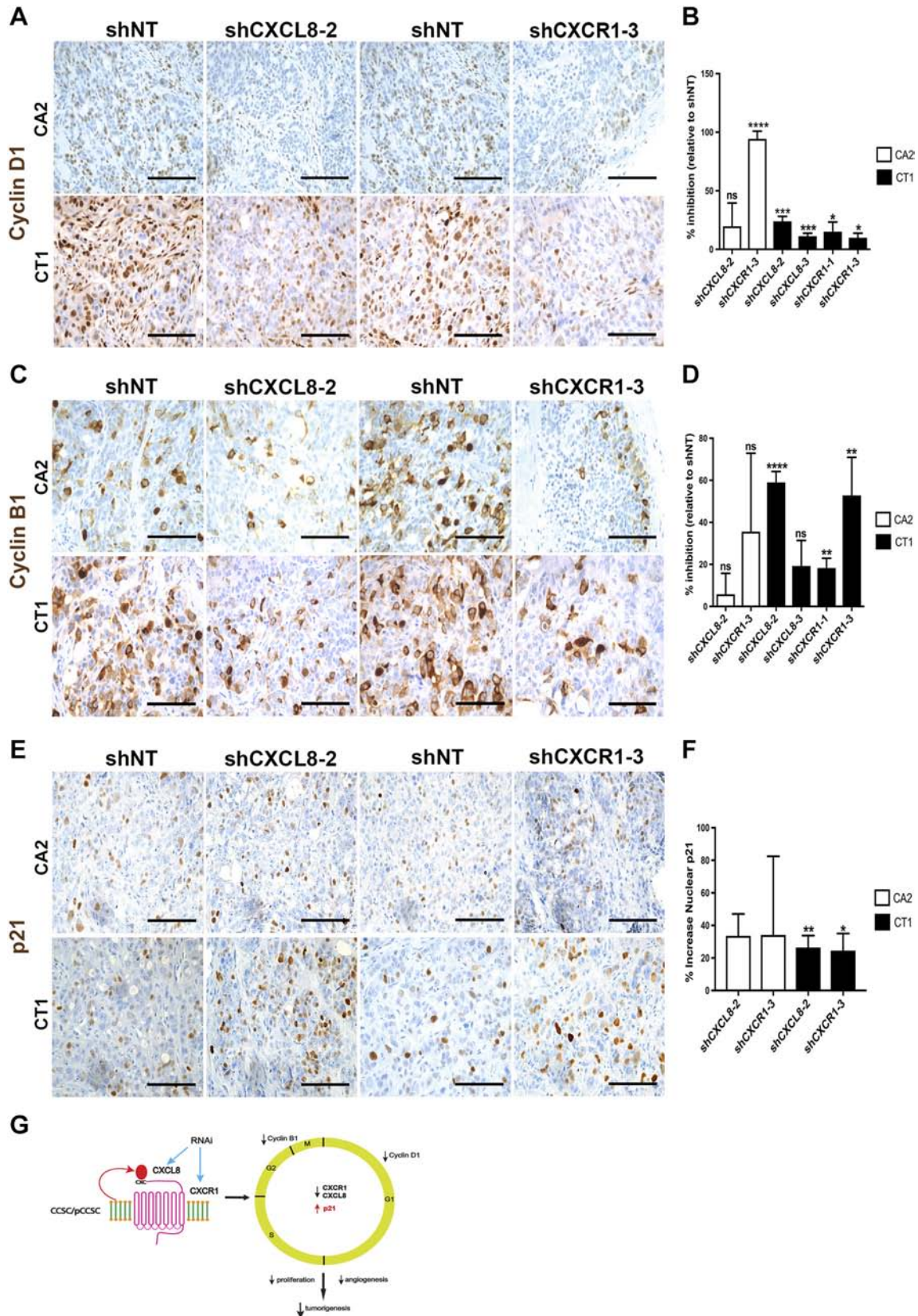
While copious evidence suggests that CXCL8 is involved or is correlated with advanced stages of colorectal cancer [30–32], the evidence for CXCL8 engagement in earlier stages of cancer is less clear [34]. Though CXCL8 has been reported as emanating from elements of the inflammatory or tumor microenvironment, we demonstrate for the first time the functional significance of both the secretion and autocrine circuit-induced responsiveness within both the sporadic colon cancer stem cells and the colitis-derived cancer stem cells. High-level expression of CXCL8 and the CCSC stem cell marker, ALDH1, was determined to significantly correlate with poor patient survival in colon cancer (Figure 1E). In contrast, high-level CXC1 expression exhibited a correlative trend for colon cancer patient survival (Figure 1D). Plausible explanations include the small size of the data set and the low expression levels of CXCR1 RNA that have been reported for CRC tumor cell lines [33,35]. Both factors may comprise the value of RNA expression-based data sets for determining the significance of CXCR1 expression for predicting colon cancer patient survival. The mechanism of how the expression of CXCL8 and CXCR1 is activated during CRC and UC is unclear but is thought to involve DNA damaging compounds emanating from the microenvironment triggering pathways leading to the activation of NF-KB, a transcriptional activator of CXCL8 and CXCR1 expression [36–38].

Our data demonstrating a functional role for autocrine CXCL8-CXCR1 signaling in both sporadic CRC and CAC is consistent with previous studies reporting similar results for prostate cancer and melanoma [27,39,40]. In contrast to our focus on using long-term, self-renewing sporadic CCSC and colitic CCSC models, other groups have used cancer cell line models, which are more comparable to tumor transient transamplifying cells which have been shown by others to have limited or absent self-renewing capacity and are only capable of generating primary tumors [11,25]. To date, several investigators have reported that CRC cell line models demonstrate CXCL8-induced cell migration [41,42]. However, there are conflicting results regarding the potential of the CRC cell lines to proliferate in response to CXCL8. Here, we show that both CCSCs and pCCSCs display a dose responsiveness to exogenous CXCL8, and fail to proliferate in response to endogenous CXCL8 when expression of either CXCL8 or CXCR1 is reduced (Figures 2 and 4, A–C, E and F).

Since both our *in vitro* and *in vivo* studies demonstrated that reducing expression of either CXCL8 or CXCR1 affected cell proliferation, we examined the effect of the CXCL8 and CXCR1 knockdowns on the cell cycle. The expression of cyclins D1 and B1 were decreased in both the CXCL8- and CXCR1- knockout tumor xenografts (Figure 6, A–D), which is consistent with a partial blockade of G1 and G2/M progression. Reduced levels of cyclin D1 are known to result in suboptimal phosphorylation of Rb and thereby decrease the transcription of E2F-dependent genes, which are required for G1 to S progression, including DNA synthesis [43,44]. Similar results have been reported for RNA interference studies knocking down CXCL8 and CXCR1 in prostate cancer cell lines [27,28]. These studies presented data that the G1 blockade correlated with a decrease in Rb phosphorylation, and collectively resulted in apoptosis. Furthermore, this group also noted decreased tumor growth and angiogenic activity in their CXCR1 knockdown tumors. We and others have detected an increase in p21, a known inducer of apoptosis and senescence (Figure 6, E and F) [27,28]. The inverse relationship between cyclin B1 and p21 is consistent with evidence demonstrating that cyclin B1-CDK1 complexes are able to sequester p21 and promote degradation [45].

We have delineated the role and functional significance of the CXCL8-CXCR1 ligand/receptor pair in the establishment of tumorigenic growth initiated by sporadic colon cancer and colitis-associated cancer stem cells. The strength of our studies include the use of primary sporadic CCSC and colitic CCSC sphere isolates to uncover the etiology of deregulated growth control resulting in CRC and CAC tumor initiation and progression. Weaknesses include the limited number of patient samples that we have examined especially in terms of defining the clinical significance of high CXCR1 expression. In addition, our mechanistic experiments addressing downstream targets of the CXCL8-CXCR1 signaling axis were limited in scope. Nonetheless, our research findings represent the most convincing study to date using primary colon cancer stem cell line models that autocrine CXCL8-CXCR1 signaling is an important driver of tumorigenesis by deregulating both cell cycle control and angiogenesis.

Conclusions

In this study, we showed for the first time that CXCL8-CXCR1 autocrine signaling regulates colon cancer tumorigenicity initiated by patient-derived CCSCs. Immunochemical and ELISA analysis demonstrated overexpression of CXCR1 and CXCL8 levels in CRC and UC patient samples confirming the clinical significance of our study. Initial *in vitro* proliferation assays validated the CXCL8 responsiveness of our model sporadic CCSCs and colitic CCSCs. Knocking down CXCR1 and CXL8 in CCSC and pCCSCs reduced *in vitro* proliferation and angiogenetic activity. *In vivo* studies measuring long-term CCSC activity demonstrated reduced tumorigenicity initiated by CXCL8 and CXCR1 knockdown

Figure 6. Knockdown of CXCL8 or CXCR1 expression in CA2 CCSCs and CT1 CCSCs disrupts regulation of the cell cycle in tumor xenografts. **A.** Immunochemical detection of the G1 progression regulator protein, cyclin D1, in CA2 CCSCs and CT1 pCCSCs control *versus* shCXCL8 and shCXCR1 knockdown secondary tumor xenografts. Representative stained shNT, shCXCL8–2 and shCXCR1–3 tumor sections are displayed for CA2 CCSCs (upper panels) and CT1 pCCSCs (lower panels). Cyclin D1, brown (DAB). **B.** Cyclin D1 expression was quantified and expressed as % inhibition relative to shNT. **C.** Immunochemical detection of G2/M progression regulator protein, cyclin B1, in CA2 CCSC and CT1 CCSC control *versus* shCXCL8 and shCXCR1 knockdown tumor xenografts. Representative stained shNT, shCXCL8–2 and shCXCR1–3 tumor sections are displayed for CA2 CCSCs (upper panels) and CT1 CCSCs (lower panels). Cyclin B1, brown (DAB). **D.** Cyclin B1 expression was quantified; expressed as % inhibition relative to shNT. **E.** Immunochemical detection of cell cycle negative regulator protein, p21, in CA2 CCSC and CT1 CCSCs control *versus* shCXCL8 and shCXCR1 knockdown secondary tumor xenografts. Representative stained shNT, shCXCL8–2 and shCXCR1–3 tumor sections are displayed for CA2 CCSCs and CT1 CCSCs. p21, brown (DAB). **F.** Expression of p21 was quantified and expressed as % increase relative to shNT. **G**. Model: Long-term CCSCs and CCSCs utilize autocrine CXCL8-CXCR1 signaling to sustain tumorigenesis. Knocking down either CXCL8 or CXCR1 inhibited tumor growth due to reduced levels of proliferation and angiogenesis. The reduction of cell cycle regulators, cyclin D1 and cyclin B1 along with an increase in p21 suggest that cell cycle progression is dysfunctional in CXCL8 and CXCR1 knockdown tumors. Open bars: CA2 CCSCs, Filled bars: CT1 CCSCs; Mean +/− SD, n = 3 (except for F, CA2 CCSC knockdown tumors, *n* = 2); *P < .05, **P < .01, ***P < .001, ****P < .0001, ns (not significant). Scale bars, 100 μm.

sporadic CCSCs and colitic CCSCs. Reduced expression of markers associated with cell proliferation, cell cycle progression and angiogenesis by CXCR1 and CXCL8 knockdown tumor xenograft suggested that CXC8-CXCR1-induced cell cycle progression and CXCL8-mediated angiogenesis are essential during tumor growth.

Supplementary data to this article can be found online at https://doi.org/10.1016/j.neo.2018.12.007.

Conflict of Interests
All authors declare no conflict of interest.

Author Contributions
R.C.F.: conception and design; methodology development, collection and/or assembly of data, data analysis and interpretation and manuscript writing; K.B, L.A.M. and S.X.: collection and/or assembly of data, data analysis and interpretation, D.L.: data analysis and interpretation; S.K.S. and S.C.: collection and/or assembly of data, data analysis and interpretation; A.B.: collection and/or assembly of data; M.L.J. and D.H.: methodology development; S. C.: collection and/or assembly of data; A.A, H.D.A. and E.W.S.: data analysis and interpretation; E.H.H.: conception and design, financial support, provision of study materials or patients, methodology development, data analysis and interpretation, manuscript writing and final approval of manuscript.

CRediT authorship contribution statement
Robert C. Fisher: Conceptualization, Methodology, Data curation, Formal analysis, Writing - original draft. **Kishan Bellamkonda:** Data curation, Formal analysis. **L. Alex Molina:** Data curation, Formal analysis. **Shao Xiang:** Data curation, Formal analysis. **David Liska:** Formal analysis. **Samaneh K. Sarvestani:** Data curation, Formal analysis. **Susmita Chakrabarti:** Data curation, Formal analysis. **Annamarie Berg:** Data curation. **Marda L. Jorgensen:** Methodology. **Denise Hatala:** Methodology. **Sugong Chen:** Data curation. **Alexandra Aiello:** Formal analysis. **Henry D. Appelman:** Formal analysis. **Edward W. Scott:** Formal analysis. **Emina H. Huang:** Conceptualization, Funding acquisition, Resources, Methodology, Formal analysis, Writing - original draft, Project administration.

Acknowledgements

References

[1]   Lasry A, Zinger A, and Ben-Neriah Y (2016). Inflammatory networks underlying colorectal cancer. *Nat Immunol* **17**, 230–240.

[2]   Hanahan D and Weinberg RA (2011). Hallmarks of cancer: the next generation. *Cell* **144**, 646–674.

[3]   Ullman TA and Itzkowitz SH (2011). Intestinal inflammation and cancer. *Gastroenterology* **140**, 1807–1816.

[4]   Fearon ER and Vogelstein B (1990). A genetic model for colorectal tumorigenesis. *Cell* **61**, 759–767.

[5]   Markowitz SD and Bertagnolli MM (2009). Molecular origins of cancer: Molecular basis of colorectal cancer. *N Engl J Med* **361**, 2449–2460.

[6]   Dalerba P, Dylla SJ, Park IK, Liu R, Wang X, Cho RW, Hoey T, Gurney A, Huang EH, and Simeone DM, et al (2007). Phenotypic characterization of human colorectal cancer stem cells. *Proc Natl Acad Sci U S A* **104**, 10158–10163.

[7]   O'Brien CA, Pollett A, Gallinger S, and Dick JE (2007). A human colon cancer cell capable of initiating tumour growth in immunodeficient mice. *Nature* **445**, 106–110.

[8]   Ricci-Vitiani L, Lombardi DG, Pilozzi E, Biffoni M, Todaro M, Peschle C, and De Maria R (2007). Identification and expansion of human colon-cancer-initiating cells. *Nature* **445**, 111–115.

[9]   Huang EH, Hynes MJ, Zhang T, Ginestier C, Dontu G, Appelman H, Fields JZ, Wicha MS, and Boman BM (2009). Aldehyde dehydrogenase 1 is a marker for normal and malignant human colonic stem cells (SC) and tracks SC overpopulation during colon tumorigenesis. *Cancer Res* **69**, 3382–3389.

[10] Carpentino JE, Hynes MJ, Appelman HD, Zheng T, Steindler DA, Scott EW, and Huang EH (2009). Aldehyde dehydrogenase-expressing colon stem cells contribute to tumorigenesis in the transition from colitis to cancer. *Cancer Res* **69**, 8208–8215.

[11] Shenoy AK, Fisher RC, Butterworth EA, Pi L, Chang LJ, Appelman HD, Chang M, Scott EW, and Huang EH (2012). Transition from colitis to cancer: high Wnt activity sustains the tumor-initiating potential of colon cancer stem cell precursors. *Cancer Res* **72**, 5091–5100.

[12] Vermeulen L, Todaro M, de Sousa Mello F, Sprick MR, Kemper K, Perez Alea M, Richel DJ, Stassi G, and Medema JP (2008). Single-cell cloning of colon cancer stem cells reveals a multi-lineage differentiation capacity. *Proc Natl Acad Sci U S A* **105**, 13427–13432.

[13] Ha H, Debnath B, and Neamati N (2017). Role of the CXCL8-CXCR1/2 Axis in Cancer and Inflammatory Diseases. *Theranostics* **7**, 1543–1588.

[14] Joseph PR, Sarmiento JM, Mishra AK, Das ST, Garofalo RP, Navarro J, and Rajarathnam K (2010). Probing the role of CXC motif in chemokine CXCL8 for high affinity binding and activation of CXCR1 and CXCR2 receptors. *J Biol Chem* **285**, 29262–29269.

[15] Sarmiento J, Shumate C, Suetomi K, Ravindran A, Villegas L, Rajarathnam K, and Navarro J (2011). Diverging mechanisms of activation of chemokine receptors revealed by novel chemokine agonists. *PLoS One* **6**e27967.

[16] Becker MD, O'Rourke LM, Blackman WS, Planck SR, and Rosenbaum JT (2000). Reduced leukocyte migration, but normal rolling and arrest, in interleukin-8 receptor homologue knockout mice. *Invest Ophthalmol Vis Sci* **41**, 1812–1817.

[17] Chen S, Fisher RC, Signs S, Molina LA, Shenoy AK, Lopez MC, Baker HV, Koomen JM, Chen Y, and Gittleman H, et al (2017). Inhibition of PI3K/Akt/mTOR signaling in PI3KR2-overexpressing colon cancer stem cells reduces tumor growth due to apoptosis. *Oncotarget* **8**, 50476–50488.

[18] Signs SA, Fisher RC, Tran U, Chakrabarti S, Sarvestani SK, Xiang S, Liska D, Roche V, Lai W, and Gittleman HR, et al (2018). Stromal miR-20a controls paracrine CXCL8 secretion in colitis and colon cancer. *Oncotarget* **9**, 13048–13059.

[19] Remmele W and Stegner HE (1987). Recommendation for uniform definition of an immunoreactive score (IRS) for immunohistochemical estrogen receptor detection (ER-ICA) in breast cancer tissue. *Pathologe* **8**, 138–140.

[20] Rhodes DR, Yu J, Shanker K, Deshpande N, Varambally R, Ghosh D, Barrette T, Pandey A, and Chinnaiyan AM (2004). ONCOMINE: a cancer microarray database and integrated data-mining platform. *Neoplasia* **6**, 1–6.

[21] Ginestier C, Liu S, Diebel ME, Korkaya H, Luo M, Brown M, Wicinski J, Cabaud O, Charafe-Jauffret E, and Birnbaum D, et al (2010). CXCR1 blockade selectively targets human breast cancer stem cells in vitro and in xenografts. *J Clin Invest* **120**, 485–497.

[22] Li A, Dubey S, Varney ML, Dave BJ, and Singh RK (2003). IL-8 directly enhanced endothelial cell survival, proliferation, and matrix metalloproteinases production and regulated angiogenesis. *J Immunol* **170**, 3369–3376.

[23] Li A, Varney ML, Valasek J, Godfrey M, Dave BJ, and Singh RK (2005). Autocrine role of interleukin-8 in induction of endothelial cell proliferation, survival, migration and MMP-2 production and angiogenesis. *Angiogenesis* **8**, 63–71.

[24] Arnaoutova I, George J, Kleinman HK, and Benton G (2009). The endothelial cell tube formation assay on basement membrane turns 20: state of the science and the art. *Angiogenesis* **12**, 267–274.

[25] Dieter SM, Ball CR, Hoffmann CM, Nowrouzi A, Herbst F, Zavidij O, Abel U, Arens A, Weichert W, and Brand K, et al (2011). Distinct types of tumor-initiating cells form human colon cancer tumors and metastases. *Cell Stem Cell* **9**, 357–365.

[26] Lim S and Kaldis P (2013). Cdks, cyclins and CKIs: roles beyond cell cycle regulation. *Development* **140**, 3079–3093.

[27] Shamaladevi N, Lyn DA, Escudero DO, and Lokeshwar BL (2009). CXC receptor-1 silencing inhibits androgen-independent prostate cancer. *Cancer Res* **69**, 8265–8274.

[28] Singh RK and Lokeshwar BL (2009). Depletion of intrinsic expression of Interleukin-8 in prostate cancer cells causes cell cycle arrest, spontaneous apoptosis and increases the efficacy of chemotherapeutic drugs. *Mol Cancer* **8**, 57.

[29] Besson A, Dowdy SF, and Roberts JM (2008). CDK inhibitors: cell cycle regulators and beyond. *Dev Cell* **14**, 159–169.

[30] Oladipo O, Conlon S, O'Grady A, Purcell C, Wilson C, Maxwell PJ, Johnston PG, Stevenson M, Kay EW, and Wilson RH, et al (2011). The expression and prognostic impact of CXC-chemokines in stage II and III colorectal cancer epithelial and stromal tissue. *Br J Cancer* **104**, 480–487.

[31] Terada H, Urano T, and Konno H (2005). Association of interleukin-8 and plasminogen activator system in the progression of colorectal cancer. *Eur Surg Res* **37**, 166–172.

[32] Ueda T, Shimada E, and Urakawa T (1994). Serum levels of cytokines in patients with colorectal cancer: possible involvement of interleukin-6 and interleukin-8 in hematogenous metastasis. *J Gastroenterol* **29**, 423–429.

[33] Adalsteinsson VA, Tahirova N, Tallapragada N, Yao X, Campion L, Angelini A, Douce TB, Huang C, Bowman B, and Williamson CA, et al (2013). Single cells from human primary colorectal tumors exhibit polyfunctional heterogeneity in secretions of ELR+ CXC chemokines. *Integr Biol (Camb)* **5**, 1272–1281.

[34] Gibson P and Rosella O (1995). Interleukin 8 secretion by colonic crypt cells in vitro: response to injury suppressed by butyrate and enhanced in inflammatory bowel disease. *Gut* **37**, 536–543.

[35] Samuel T, Fadlalla K, Gales DN, Putcha BD, and Manne U (2014). Variable NF-kappaB pathway responses in colon cancer cells treated with chemotherapeutic drugs. *BMC Cancer* **14**, 599.

[36] Mariani F, Sena P, and Roncucci L (2014). Inflammatory pathways in the early steps of colorectal cancer development. *World J Gastroenterol* **20**, 9716–9731.

[37] Maxwell PJ, Gallagher R, Seaton A, Wilson C, Scullin P, Pettigrew J, Stratford IJ, Williams KJ, Johnston PG, and Waugh DJ (2007). HIF-1 and NF-kappaB-mediated upregulation of CXCR1 and CXCR2 expression promotes cell survival in hypoxic prostate cancer cells. *Oncogene* **26**, 7333–7345.

[38] Stein B and Baldwin Jr AS (1993). Distinct mechanisms for regulation of the interleukin-8 gene involve synergism and cooperativity between C/EBP and NF-kappa B. *Mol Cell Biol* **13**, 7191–7198.

[39] Araki S, Omori Y, Lyn D, Singh RK, Meinbach DM, Sandman Y, Lokeshwar VB, and Lokeshwar BL (2007). Interleukin-8 is a molecular determinant of androgen independence and progression in prostate cancer. *Cancer Res* **67**, 6854–6862.

[40] Singh S, Sadanandam A, Varney ML, Nannuru KC, and Singh RK (2010). Small interfering RNA-mediated CXCR1 or CXCR2 knock-down inhibits melanoma tumor growth and invasion. *Int J Cancer* **126**, 328–336.

[41] Ning Y, Manegold PC, Hong YK, Zhang W, Pohl A, Lurje G, Winder T, Yang D, LaBonte MJ, and Wilson PM, et al (2011). Interleukin-8 is associated with proliferation, migration, angiogenesis and chemosensitivity in vitro and in vivo in colon cancer cell line models. *Int J Cancer* **128**, 2038–2049.

[42] Sturm A, Baumgart DC, d'Heureuse JH, Hotz A, Wiedenmann B, and Dignass AU (2005). CXCL8 modulates human intestinal epithelial cells through a CXCR1 dependent pathway. *Cytokine* **29**, 42–48.

[43] Dyson N (1998). The regulation of E2F by pRB-family proteins. *Genes Dev* **12**, 2245–2262.

[44] Nevins JR (1998). Toward an understanding of the functional complexity of the E2F and retinoblastoma families. *Cell Growth Differ* **9**, 585–593.

[45] Kreis NN, Friemel A, Zimmer B, Roth S, Rieger MA, Rolle U, Louwen F, and Yuan J (2016). Mitotic p21Cip1/CDKN1A is regulated by cyclin-dependent kinase 1 phosphorylation. *Oncotarget* **7**, 50215–50228.